Pyridoimidazolones as Novel Potent Inhibitors of v-Raf Murine Sarcoma Viral Oncogene Homologue B1 (BRAF)

Dan Niculescu-Duvaz,[†] Catherine Gaulon,[†] Harmen P. Dijkstra,[†] Ion Niculescu-Duvaz,[†] Alfonso Zambon,[†] Delphine Ménard,[†] Bart M. J. M. Suijkerbuijk,[†] Arnaud Nourry,[†] Lawrence Davies,[†] Helen Manne,[†] Frank Friedlos,[†] Lesley Ogilvie,[†] Douglas Hedley,[†] Steven Whittaker,[‡] Ruth Kirk,[‡] Adrian Gill,[§] Richard D. Taylor,[§] Florence I. Raynaud,[†] Javier Moreno-Farre,[†] Richard Marais,[‡] and Caroline J. Springer*[,†]

Cancer Research UK Centre for Cancer Therapeutics, The Institute of Cancer Research, 15 Cotswold Road, Sutton, Surrey SM2 5NG, U.K., Cancer Research UK Centre for Cell and Molecular Biology, The Institute of Cancer Research, 237 Fulham Road, London SW3 6JB, U.K., and Astex Therapeutics Ltd., Registered in England at 436 Cambridge Science Park, Cambridge CB4 0QA, U.K.

Received December 1, 2008

BRAF is a serine/threonine kinase that is mutated in a range of cancers, including 50−70% of melanomas, and has been validated as a therapeutic target. We have designed and synthesized mutant BRAF inhibitors containing pyridoimidazolone as a new hinge-binding scaffold. Compounds have been obtained which have low nanomolar potency for mutant BRAF (12 nM for compound **5i**) and low micromolar cellular potency against a mutant BRAF melanoma cell line, WM266.4. The series benefits from very low metabolism, and pharmacokinetics (PK) that can be modulated by methylation of the NH groups of the imidazolone, resulting in compounds with fewer H-donors and a better PK profile. These compounds have great potential in the treatment of mutant BRAF melanomas.

Introduction

RAF[a] (so named from the v-raf oncogene that causes rapidly growing fibrosarcomas in mice[1]) is a serine/threonine kinase that is part of the mitogen-activated protein kinase (MAPK) signal transduction cascade: RAF-MAPK/ERK kinase (MEK)-extracellular regulated kinase (ERK) that regulates cell growth, differentiation, and proliferation in response to external stimuli such as growth factors.[2] Following RAF activation, the cascade is stimulated and MEK and ERK are sequentially phosphorylated and activated. ERK then regulates cell function by phosphorylating more than 50 substrates in the cytosol and the nucleus.[3] There are three members of the RAF family (ARAF, BRAF and CRAF). BRAF is mutated in approximately 2% of human cancers, with particularly high frequencies in melanoma (50−70%), ovarian (35%), thyroid (30%), and colorectal (10%) cancers.[4,5] The most common mutation (90%) is a valine for glutamic acid substitution at position 600, termed ^{V600E}BRAF. ^{V600E}BRAF shows a permanent 500-fold elevated kinase activity.[6] In addition, ^{V600E}BRAF stimulates constitutive ERK signaling in mammalian cells[4,7,8] and it transforms established cells, allowing them to grow as tumors in nude mice.[4,7] In melanoma, ^{V600E}BRAF stimulates proliferation and survival; inhibition of BRAF signaling with siRNA inhibits proliferation and induces apoptosis.[9,10] These data validate BRAF as an important and exciting therapeutic target in human cancer. Inhibitors of RAF have been developed, such as PLX4032,[11] RAF265[12] and XL-281[13] for BRAF and sorafenib for CRAF (Figure 1). Sorafenib (launched for renal cell carcinoma [RCC][14]) failed to show therapeutic activity in the treatment of malignant melanoma,[15] presumably because of its poor cellular activity against ^{V600E}BRAF. RAF265, PLX4032 and XL-281 are in phase 1 clinical trials, the first two for melanoma, but no results have been reported yet. Therefore, ^{V600E}BRAF inhibitors are of great topical interest currently.

We initiated a new series of BRAF inhibitors to improve upon sorafenib in terms of both ^{V600E}BRAF potency and cell growth inhibition. For this purpose, we have discovered a new hinge-binding group, pyridoimidazolone, as a key structural element of our new series of ^{V600E}BRAF inhibitors.

Most kinase inhibitors bind into the adenosine triphosphate (ATP) pocket and form interactions with the hinge separating the two lobes of the kinase domain. The hinge binds to the adenine group of ATP, through generation of a network of H-bonds. This motif has been targeted in the design of most kinase inhibitors, which contain hydrogen bond accepting and donating groups that can form noncovalent interactions with the hinge essential for the potency of inhibition. Many heterocyclic groups have been used as hinge-binding moieties to generate interactions with the backbone of the hinge, for example a 2-carboxamidopyridine group in sorafenib or a 4-aminoquinazoline group in gefitinib and erlotinib.[16] We implemented the bicyclic pyridoimidazolones as a novel hinge-binding group in the design of new BRAF inhibitors. The imidazolone moiety was envisaged as having two purposes: affording two interactions with the hinge backbone, one due to the pyridine nitrogen H-bond acceptor and the other *via* the 3-NH donor of the imidazolone. In addition, projecting a hydrophilic "edge" of the inhibitors toward the aqueous solvent was envisaged as favorable. The imidazolone ring is also rigid, and reduces the number of rotatable bonds compared to the methylcarboxamide group of sorafenib. Reducing the number of rotatable bonds can be desirable for improved PK properties.[17]

We combined our pyridoimidazolone hinge binding group with a pharmacophore known to engender type II kinase

* To whom correspondence should be addressed. Phone: +44 20 8722 4214. Fax: +44 20 8722 4046. E-mail: caroline.springer@icr.ac.uk.

[†] Cancer Research UK Centre for Cancer Therapeutics, The Institute of Cancer Research.

[‡] Cancer Research UK Centre for Cell and Molecular Biology, The Institute of Cancer Research.

[§] Astex Therapeutics Ltd.

[a] Abbreviations: RAF, rapidly growing fibrosarcoma; BRAF, V-RAF murine sarcoma viral oncogene homologue B1; MAPK, mitogen-activated protein kinase; MEK, MAPK/ERK kinase; ERK, extracellular regulated kinase; PK, pharmacokinetics; Boc, *tert*-butoxycarbonyl; DMF, dimethylformamide; TFA, trifluoroacetic acid; THF, tetrahydrofuran; DCM, dichloromethane; iv, intravenous; SAR, structure−activity relationship.

10.1021/jm801509w CCC: $40.75
Published on Web 03/26/2009

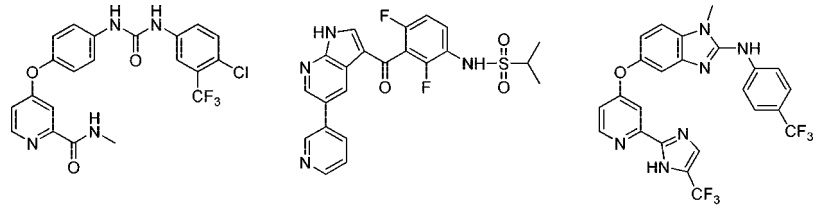

Figure 1. Structures of RAF inhibitors sorafenib, PLX4032 and RAF265.

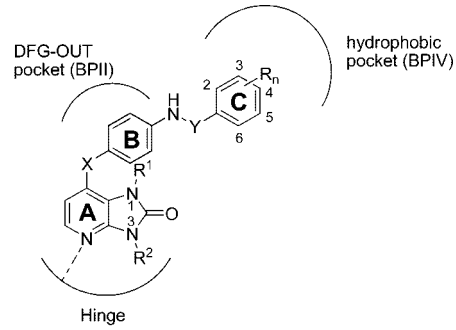

Figure 2. General structure of the pyridoimidazolone-based BRAF inhibitors described in this paper.

inhibitors. Type II kinase inhibitors occupy a hydrophobic pocket adjacent to the ATP pocket and the gatekeeper residue, created by the displacement of the DFG loop. Type II inhibitors bind to a DFG-out or inactive conformation.[18] Sorafenib is an example of an inhibitor of the DFG-out conformation. Our cocrystal structure of sorafenib with BRAF supports this binding mode.[19] The pharmacophore of type II kinase inhibitors consists of a hinge-binding moiety linked to an aromatic/heteroaromatic ring in the DFG-out pocket (BPII), a hydrogen bond donor/acceptor and usually a lipophilic group in the pockets created by the displacement of the DFG loop (BPIII and BPIV).[18]

The general structure of the inhibitors shown in Figure 2 fits this model: the pyridoimidazolone hinge-binder (ring A) is connected through an oxygen or a sulfur atom to the phenyl ring B that is expected to occupy the DFG-out pocket (BPII). Rings B and C are connected *via* the H-donor/acceptor linker B−C. Urea is a linker frequently used in type II inhibitors, for example in sorafenib where it interacts with Glu501 and the backbone of Asp594. Different H-donor/acceptor linkers were also explored, e.g., thiourea, amide and sulfonamide. The substituted phenyl ring C occupies the BPIV pocket in the generalized kinase model, with the lipophilic substituent targeting the BPIII pocket.

Chemistry

The structure of the inhibitors can be rationalized to 3 domains: the novel bicyclic hinge-binding pyridoimidazolone (ring A), the phenyl ring in the DFG-out pocket (ring B) and the aromatic group occupying the BPIV pocket (ring C) (Figure 2). Rings A and B are interconnected through either an O or an S. The linker between rings B and C plays two critical roles, in binding to Glu501 and in positioning the C ring in the DFG pocket. We utilized the 1,3-disubstituted urea pharmacophore as the B−C linker, since it was described as being effective in interacting with Glu501 *via* both NH groups.[19] We also explored several alternatives, such as amides, sulfonamides, thioureas and methyleneamides.

Two synthetic routes were developed. In route I, described in Scheme 1, ring C is first coupled to 4-(4-aminophenoxy)-3-nitropyridin-2-amine **2**, whereafter the imidazolone is formed in the last step. This route was used to obtain compound **5a**. In route II, the imidazolone is formed initially to generate the complete ring A−ring B part of the inhibitors (the common intermediate, for example compound **9** in Scheme 2) containing an amino group that can be reacted in the last step with a variety of electrophiles. This second route is more suitable to explore quickly a range of different C-rings and B−C linkers in a parallel fashion, since there is just one step from the common intermediate to the final product. This method was adopted for the synthesis of the rest of the BRAF inhibitors described here (**5b**−**x**, **26**, **27a**−**f**, **28a**−**e**, **29a**−**g**).

The starting material for both routes is 2-amino-4-chloro-3-nitropyridine **1**. The chlorine atom can be substituted selectively with the 4-aminophenolate, whereby the phenolate is preferred to the amine as nucleophile, to afford 4-(4-aminophenoxy)-3-nitropyridin-2-amine **2**.

Route 1. The amino group on the phenyl B-ring is more nucleophilic than the one in position 2 of the pyridine (which is deactivated both by the 3-nitro group and the pyridyl ring), and can be reacted selectively with 4-chloro-3-trifluoromethylphenyl isocyanate to afford urea **3**. Reduction of the nitro group and cyclization of the diamino compound **4** with triphosgene afforded the target product **5a** (Scheme 1).

Route 2. For the synthesis of the common intermediate **9**, 4-(4-aminophenoxy)-3-nitro-2-aminopyridine **2** is protected selectively with *tert*-butoxycarbonyl (Boc) at the 4-aminophenoxy group, the nitro group is subsequently reduced and the resulting diamino compound **7** is reacted with phosgene to afford compound **8**. Intermediate **6** can also be obtained by direct coupling of 2-amino-4-chloro-3-nitropyridine **1** with 4-*N*-Boc-aminophenol. Subsequent deprotection with trifluoroacetic acid (TFA) generates common intermediate **9** (Scheme 2). The Boc protection-deprotection is required to avoid side reactions of the 4-amino group on ring B with phosgene.

We wished to investigate the importance of the two NH groups of the imidazolone, with N3 being expected to be involved in hinge-binding. We hypothesized that substitution of N1 or N3 or both nitrogen atoms of the imidazolone with a methyl or ethyl group would be useful in answering this question. Also, alkylation of one or both imidazolone NH groups would remove one or two H-donors, yielding compounds that would be more orally bioavailable. For this purpose, the intermediates **16** (Scheme 3), **20**, **20a** (Scheme 4) and **21** (Scheme 5) were synthesized.

The synthesis of common intermediate **16**, methylated at the N3 of the imidazolone, is shown in Scheme 3. The methylated starting material 4-chloro-3-nitro-2-methylaminopyridine **12** is

Scheme 1. Synthetic Route I: Synthesis of Compound **5a**[a]

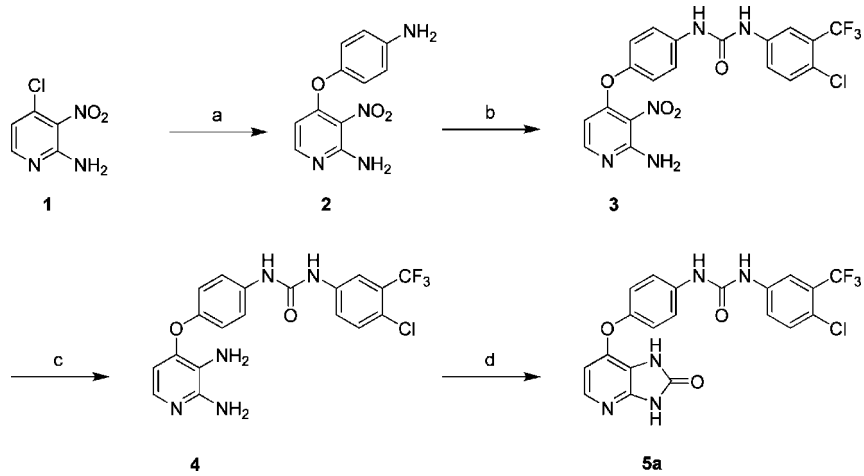

[a] Reagents and conditions: (a) 4-amino-phenol, *t*-BuOK, DMF, 80 °C; (b) 4-chloro-3-trifluoromethylphenyl isocyanate, THF; (c) H_2, Pd/C, EtOH; (d) triphosgene, NEt_3, THF.

Scheme 2. Synthesis of Unsubstituted Imidazolone Intermediate **9**[a]

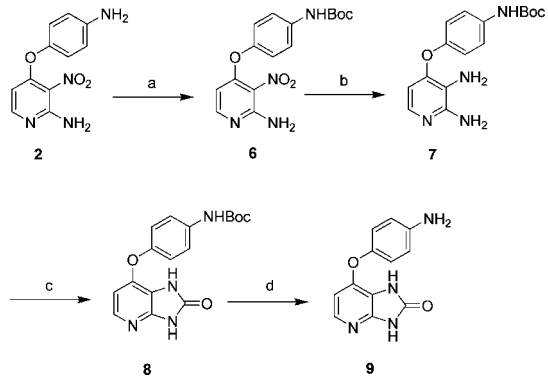

[a] Reagents and conditions: (a) Boc_2O, THF; (b) H_2, Pd/C, EtOH; (c) $COCl_2$, pyridine, THF; (d) TFA.

obtained from **1** in a three-step procedure: protection of the amino group with Boc, methylation with methyl iodide (MeI) and sodium hydride (NaH) and Boc deprotection. Although longer than the single step direct methylation of 4-chloro-3-nitro-2-aminopyridine **1**, this method has an improved yield (>90% overall) and results in fewer impurities. Aromatic nucleophilic substitution of the 4-chloro intermediate **12** with 4-*N*-Boc-aminophenolate affords intermediate **13**, which is converted to common intermediate **16** by a method similar to that for intermediate **9** (Scheme 4).

Acylation of the diamino intermediate **7** with ethyl chloroformate occurs at the more nucleophilic 3-amino group on the pyridyl ring (corresponding to N1 of the imidazolone). In order to allow the selective methylation of N1, the Boc protecting group was removed with TFA affording intermediate **18**, which contains three amino groups, with only the 3-pyridyl nitrogen (the future N1 of the imidazolone) being modified as ethyl carbamate. Reaction with 1 equiv of NaH removes the more acidic proton of the carbamate, converting this nitrogen into a stronger nucleophile than the other two amino groups. Addition of MeI therefore selectively substitutes this position to afford intermediate **19**. Upon heating **19** in a microwave reactor with sodium ethoxide, the carbamate cyclizes to imidazolone **20** (Scheme 4), methylated at the N1 of the imidazolone.

Attempts to obtain the imidazolone dimethylated at both N1 and N3 by direct methylation of intermediate **9** with NaH and MeI produced a complex mixture of products with a variable degree of methylation. Therefore, a more selective method was employed. Dimethylated common intermediate **20a** was obtained by a similar method to intermediate **20,** starting from the monomethylated intermediate **14** (Scheme 4).

Interestingly, intermediate **21** with N1 and N3 dialkylated with ethyl groups was obtained directly from intermediate **9** by deprotonation with NaH and alkylation with ethyl iodide (Scheme 5). In this case, alkylation proceeded selectively following the deprotonation of the more acidic NH groups of the imidazolone.

Common intermediate **25** with a sulfur linker instead of oxygen between rings A and B can be synthesized in a similar manner to **9**, replacing the 4-*N*-Boc-aminophenol with 4-*N*-Boc-aminothiophenol, as illustrated in Scheme 6.

Ureas with a range of aromatic rings C were obtained from the reaction of common intermediates **9**, **16**, **20**, **20a**, **21** or **25** with aromatic isocyanates. For ureas **5d**, **5h**, **5i** and **5j**, the respective isocyanates were unavailable commercially. These compounds were obtained by reacting the common intermediates with the phenyl carbamates of the respective amines instead. Thiourea **26** was obtained from the common intermediate **9** and the corresponding isothiocyanate. Aromatic amides (**27a**−**f**) and methyleneamides (**28a**−**e**) were obtained from the common intermediates and the respective acid chlorides. Sulfonamides (**29a**−**g**) were also obtained from common intermediates and sulfonyl chlorides. The general synthesis of all the final compounds except **5a** from common intermediates is presented in Scheme 7.

Results and Discussion

Our goal was to identify potent inhibitors of BRAF based on our novel hinge-binding scaffold. The importance of the two imidazolone NH groups for the binding affinity and the linker between rings A and B was investigated, as was the structure−activity relationship (SAR) around ring C and the linker between rings B and C. Accordingly, the biological activities of compounds **5a**−**x**, **26**, **27a**−**f**, **28a**−**e**, **29a**−**g** were determined in 2 separate assays: (1) inhibition of ^{V600E}BRAF kinase activity (IC_{50} BRAF), and (2) cell growth inhibition of mutant BRAF WM266.4 melanoma cells measured by sulforhodamine-B (GI_{50} SRB).

Scheme 3. Synthesis of N3-Methylated Intermediate **16**[a]

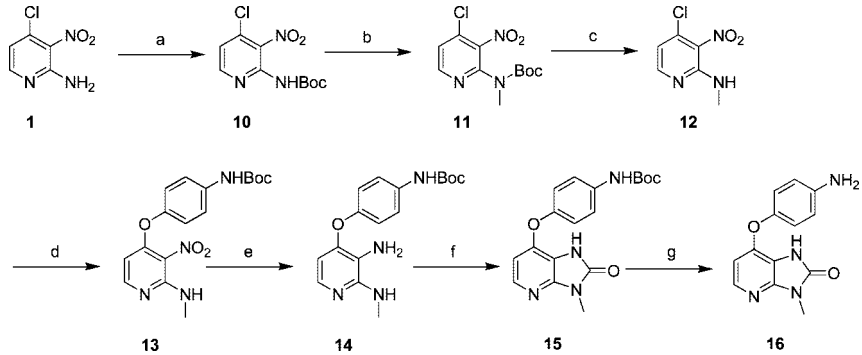

[a] Reagents and conditions: (a) Boc_2O, NaH, THF; (b) MeI, NaH, THF; (c) TFA; (d) 4-(*N*-Boc-amino)-phenol, *t*-BuOK, DMF, 70 °C; (e) H_2, Pd/C, EtOH; (f) triphosgene, pyridine, THF; (g) TFA.

Scheme 4. Synthesis of N1-Methylated and N1,N3-Dimethylated Intermediates **20** and **20a**[a]

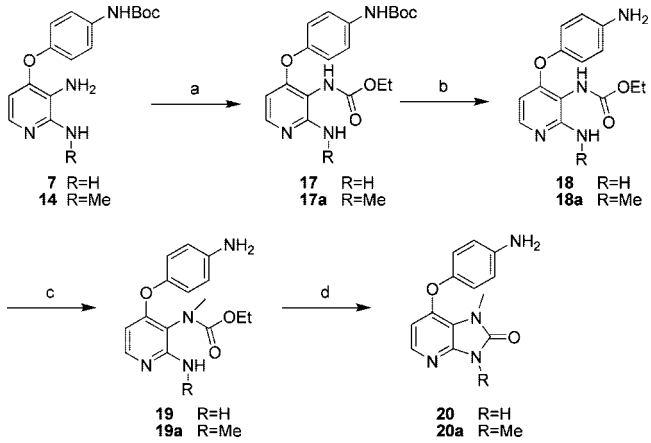

[a] Reagents and conditions: (a) EtOCOCl, pyridine, THF; (b) TFA; (c) MeI, NaH, THF; (d) EtONa, EtOH, microwave.

Scheme 5. Synthesis of Diethylated Intermediate **21**[a]

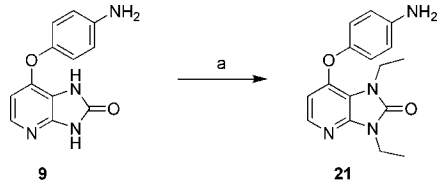

[a] Reagents and conditions: (a) EtI, NaH, DMF.

The IC_{50} and GI_{50} results are presented in Tables 1, 2 and 3.

SAR of Ring A: Imidazolone. Compound **5a** is a good inhibitor of mutant BRAF and exhibits a 2-fold improvement over sorafenib on the BRAF IC_{50} as well as a modest improvement in the cellular assay GI_{50}. Many of the synthesized compounds (see Table 1) with this new scaffold show potent BRAF inhibition and low micromolar cell growth inhibition, attesting to the ability of the pyridoimidazolone to interact with the hinge of mutant BRAF kinase.

Methylation of the N1 position of the imidazolone is tolerated, with no difference in either the BRAF IC_{50} or the SRB GI_{50} (**5o** vs **5a**). Since this nitrogen is likely to face the solvent, this result is expected. Surprisingly, the methylation of the N3 position also shows little effect, with compounds **5q** and **5s** being only slightly less potent or equipotent to their nonmethylated counterparts **5a** and **5k**, respectively. Dimethylation at both N1 and N3 of the imidazolone is also tolerated, with compound **5t** showing a less than 3-fold increase in BRAF IC_{50} and no significant difference in its SRB GI_{50} compared to its nonmethylated and monomethylated counterparts **5a**, **5o** and **5q.** In our model, the NH-3 of the imidazolone is facing the hinge backbone. However, there is apparently enough space to fit a methyl group and the NH-3 does not appear to be essential for hinge-binding. Unsurprisingly, compound **5u**, substituted with two bulkier ethyl groups at both N1 and N3 of the imidazolone, is 10-fold less active.

SAR of A−B Linker. A replacement of the oxygen linker between rings A and B with sulfur (compounds **5v**−**x**) does not have any effect on the BRAF IC_{50}, but results in a better cell growth inhibition. This is most probably due to an increased cell membrane permeability because of its increased lipophilicity.

SAR of Ring C. The initial structure of the inhibitors contains a urea linker between rings B and C, since 1,3-diarylureas have been reported to be inhibitors of kinases (e.g., in sorafenib), while the structure of the aryl ring C was varied. A relatively large and lipophilic group in the 3-position (with respect to the urea substituent) is an absolute requirement for activity. Such a group can be CF_3 (as in **5a**, **5d**,**e**, **5i**−**k**, **5n**,**o**, **5q**, **5s**−**x**), *tert*-Bu (in **5p**, **5r**) or OCF_3 (in **5h**). The BRAF IC_{50} shows a difference greater than 3 orders of magnitude between **5a** and **5c**, where the only difference is the *meta* CF_3 group. In compound **5m**, the morpholine presumably plays the role of the lipophilic group, since it is five times more potent than the corresponding compound **5l**, which lacks the morpholine group. Compounds without the lipophilic *meta* group (**5b**, **5c**) are completely devoid of activity. According to modeling, the CF_3 group fills the lipophilic pocket vacated when the DFG loop is out, corresponding to the BPIII pocket in the generalized kinase model.[18,19] The 3-position is compulsory for the CF_3 group in order to maintain activity (**5f** with CF_3 at position 2 and **5g** with CF_3 at position 4 are inactive). The second substituent on the aryl ring can contribute to an increased cellular activity. Compound **5a** has a GI_{50} (SRB) of 4.2 mM, whereas a similar compound without the Cl (**5e**) has no measurable cellular activity, despite its good potency in the BRAF assay. Similarly, a fluorine atom or a methoxy group at the 6-position leads to low micromolar cell growth inhibition (**5i**−**k**, **5s**). A chlorine atom at position 5, however, is not favorable for the activity (**5d** is 5-fold less potent than **5a**). The improved cellular activity of these compounds bearing a second or third substituent on ring C could be caused by improved cell permeability, due to increased lipophilicity (for the Cl substituent) or to the removal of an H-donor, the NH of the urea, by intramolecular H-bonding with the fluoro or methoxy substituent at the 6-position.

Scheme 6. Synthesis of Intermediate **25** with a Sulfur A−B Linker[a]

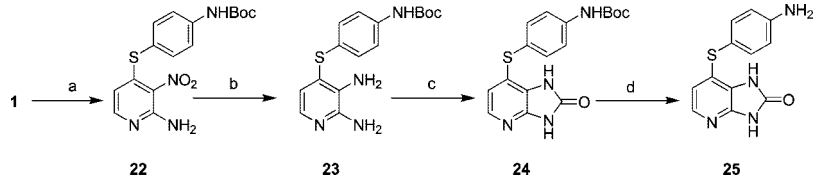

[a] Reagents and conditions: (a) 4-(*N*-Boc-amino)-benzenethiol, NaH, DMSO; (b) H_2, Raney-Ni, EtOH/AcOEt; (c) carbonyldiimidazole, THF; (d) TFA.

Scheme 7. Synthetic Route II: Synthesis of Final Compounds from Common Intermediates

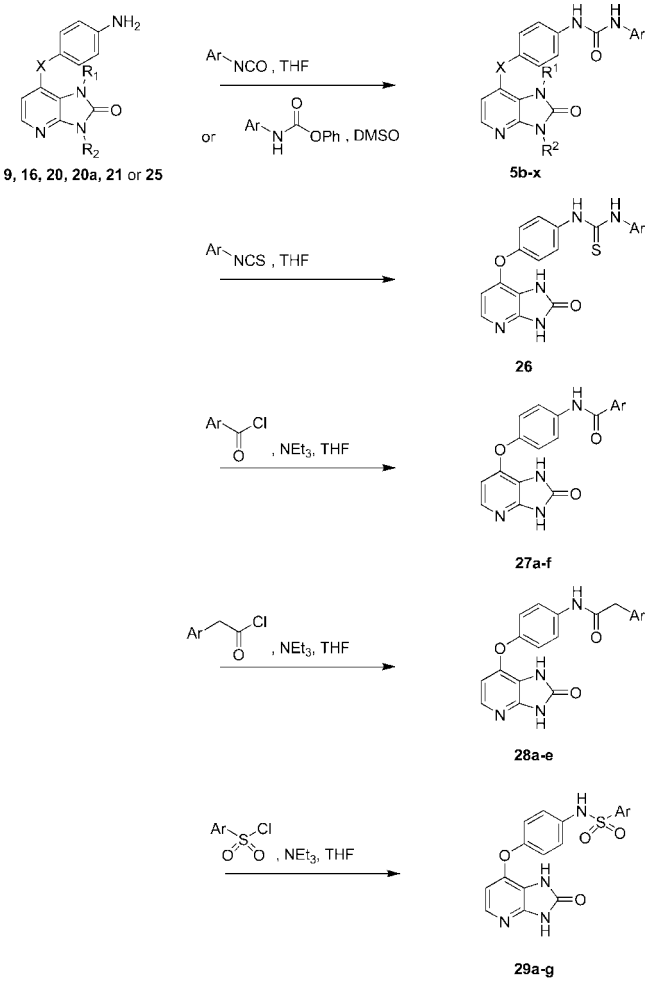

SAR of Linker B−C. Replacement of the urea group with an amide or sulfonamide group results in poor activity (**27a**−**f**, Table 2, and **29a**−**g**, Table 3). The only compound with submicromolar activity is sulfonamide **29b** with a naked phenyl group; any attempt to substitute on the phenyl ring leads to compounds with lower activity. Compound **26** is still active, but less so than the equivalent urea **5a**, in both mutant BRAF assays, therefore the thiourea provides no advantage over the urea linker. The better activity of the urea group compared to the other linkers reported could be due to the interactions of one or both of its NH-donors with Glu501,[19] or because it is orienting ring C and its 3-substituent on the correct vector toward the DFG pocket, or both. Interestingly, the methyleneamides **28d** and **28e**, which are the urea isostere equivalents of **5h** and **5e** respectively, and would present the same conformation for ring C, have no activity on BRAF. This supports the suggestion that at least the urea NH vicinal to ring C is crucial for activity.

Metabolism and PK. Four compounds were assessed for their metabolic liabilities in mouse liver microsomes (MLMs). The compounds assessed and their percentage metabolism after 30 min incubation with MLMs are **5a** (0%), **5o** (11%), **5j** (8%), **29b** (5%). Thus the metabolism of all the compounds assessed is low (<20%). PK assessments were performed on compounds **5a**, **5o** and **5q** following administration (2 mg/kg intravenous (iv)) to nude mice bearing human mutant BRAF melanoma xenografts (WM266.4). The data are summarized in Table 4. *N*-Methylation of the imidazolones greatly improves all the PK parameters (AUC, C_{max} and half-life are increased, and the clearance is reduced to levels well below that of liver blood flow).

Conclusion

A new series of potent BRAF inhibitors bearing a novel pyridoimidazolone hinge-binding group has been designed. Their synthesis, SAR and *in vivo* PK are reported here. Five compounds (**5a**, **5i**, **5j**, **5v** and **5w**) are more potent than the licensed drug sorafenib (that was designed as a RAF inhibitor) in two assays for mutant BRAF (BRAF IC_{50} and SRB GI_{50}). Up to a 4-fold improvement in BRAF IC_{50} is achieved, with a potency as low as 12 nM for compound **5i**. We hypothesize that an improvement in cellular activity compared to sorafenib of the compounds reported herein would provide beneficial therapeutic efficacy in mutant BRAF- tumors including melanoma. Compound **5v** is 4-fold more potent than sorafenib in inhibiting WM266.4 melanoma cell growth. Overall, this novel series is promising, with excellent *in vitro* potency both against the isolated mutant BRAF enzyme and in mutant BRAF driven cells. The series has low metabolism and a good PK profile that can be modulated by structural changes, warranting its assessment *in vivo* to determine whether these characteristics translate into antitumor efficacy.

Experimental Section

Materials and Methods. All starting materials, reagents and solvents for reactions were reagent grade and used as purchased. Chromatography solvents were HPLC grade and were used without further purification. Reactions were monitored by thin layer chromatography (TLC) analysis using Merck silica gel 60 F-254 thin layer plates. Flash column chromatography was carried out on Merck silica gel 60 (0.015−0.040 mm) or in disposable Isolute Flash Si and Si II silica gel columns. Preparative TLC was performed on either Macherey-Nagel [809 023] precoated TLC plates SIL G-25 UV_{254} or Analtech 2015 precoated preparative TLC plates, 2000 μm with UV_{254}. LCMS analyses were performed on a Micromass LCT/Water's Alliance 2795 HPLC system with a Discovery 5 μm, C18, 50 mm × 4.6 mm i.d. column from Supelco at a temperature of 22 °C using the following solvent systems: solvent A, methanol; solvent B, 0.1% formic acid in water at a flow rate of 1 mL/min. Gradient starting with 10% A/90% B from 0 to 0.5 min, then 10% A/90% B to 90% A/10% B from 0.5 to 6.5 min and continuing at 90% A/10% B up to 10 min. From 10 to 10.5 min the gradient reverted back to 10% A/90% B, where the concentrations remained until 12 min. UV detection was at 254

Table 1. BRAF Inhibitors with Urea or Thiourea Linker B−C

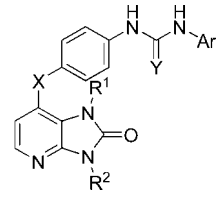

Compound	R^1	R^2	X	Y	Ar (ring C)	BRAF IC_{50} (μM)	SRB GI_{50} (μM)
sorafenib						0.043	5.0
5a	H	H	O	O	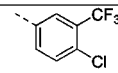	0.023	4.2
5b	H	H	O	O		>100	>100
5c	H	H	O	O	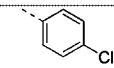	>100	>100
5d	H	H	O	O	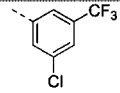	0.1	12.8
5e	H	H	O	O	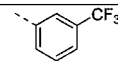	0.014	>100
5f	H	H	O	O		>100	>100
5g	H	H	O	O	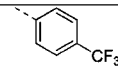	>100	>100
5h	H	H	O	O	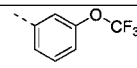	0.021	>100
5i	H	H	O	O	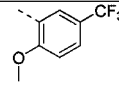	0.012	4.2
5j	H	H	O	O	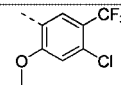	0.027	1.6
5k	H	H	O	O	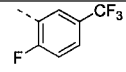	0.052	3.3
5l	H	H	O	O	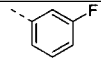	2.84	13.9
5m	H	H	O	O	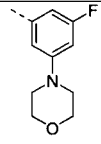	0.6	41
5n	H	H	O	O	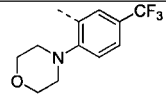	0.86	5.2
5o	Me	H	O	O	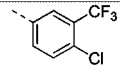	0.022	5.3

Table 1. Continued

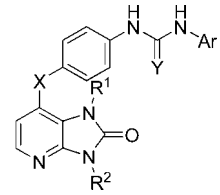

5p	Me	H	O	O	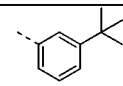	0.163	2.82
5q	H	Me	O	O	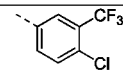	0.045	3.7
5r	H	Me	O	O	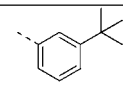	0.06	7
5s	H	Me	O	O	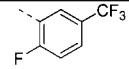	0.046	1.94
5t	Me	Me	O	O	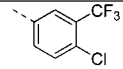	0.061	4.8
5u	Et	Et	O	O	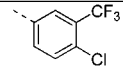	0.305	22
5v	H	H	S	O	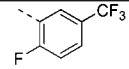	0.029	1.28
5w	H	H	S	O	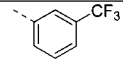	0.028	1.42
5x	H	H	S	O	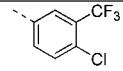	0.04	2.1
26	H	H	O	S	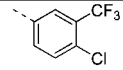	0.085	10.7

nm, and ionization was positive or negative ion electrospray. Samples were supplied as 1 mg/mL in DMSO or methanol with 3 μL injected on a partial loop fill. The purity of the final compounds was determined by HPLC as described above and is 95% or higher unless specified otherwise. NMR spectra were recorded in DMSO-d_6 on a Bruker DPX 250 MHz or a Bruker Advance 500 MHz spectrometer.

1-(4-(2,3-Dihydro-2-oxo-1*H*-imidazo[4,5-*b*]pyridin-7-yl-oxy)-phenyl)-3-(4-chloro-3-(trifluoromethyl)phenyl)urea (5a). Triphosgene (10 mg, 0.03 mmol) was added to a solution of 1-(4-(2,3-diaminopyridin-4-yl-oxy)phenyl)-3-(4-chloro-3-(trifluoromethyl)phenyl)urea (**4**) (44 mg, 0.1 mmol) and triethylamine (30 μL, 0.21 mmol) in dry THF (1 mL), cooled at 0 °C. The mixture was stirred at 0 °C for 15 min, and at room temperature for 1 h. The precipitate formed was filtered off, and the filtrate evaporated. The residue was purified by column chromatography (eluent gradient AcOEt to THF:AcOEt 1:1), to afford the title compound (11 mg, 24%). ^{1}H NMR (δ, ppm, DMSO-d_6): 6.35 (d, 1H, $H_{Py,5}$, J = 6.7 Hz), 7.14 (d, 2H, $H_{arom,Ph,3+5}$, J = 10.0 Hz), 7.54 (d, 2H, $H_{arom,Ph,2+6}$), 7.64 (bs, 2H, $H_{arom'}$), 7.77 (d, 1H, $H_{Py,6}$), 8.12 (s, 1H, $H_{arom'}$), 8.94 (s, 1H, $NH_{urea,1}$), 9.18 (s, 1H, $NH_{urea,3}$), 11.19 (s, 1H, NH_{Py3}), 11.36 (s, 1H, NH_{Py2}). LC−MS: m/z 463 (M, 100). HRMS: m/z [M + H]$^+$ calcd for $C_{20}H_{14}ClF_3N_5O_3$, 464.0737; found, 464.0739.

1-(4-(2,3-Dihydro-2-oxo-1*H*-imidazo[4,5-*b*]pyridin-7-yl-oxy)-phenyl)-3-phenyl-urea (5b). 7-(4-Amino-phenyloxy)-2,3-dihydro-2-oxo-1*H*-imidazo[4,5-*b*]pyridine (**9**) (65 mg, 0.27 mmol) was suspended in dry pyridine (3 mL) and heated at 50 °C. Phenyl isocyanate (30 μL, 0.28 mmol) was added; the reaction mixture was heated at reflux for 2 h. After cooling at room temperature, DCM (20 mL) was added, and the precipitate formed was filtered and washed with more DCM, to afford the title compound (67 mg, 69%). ^{1}H NMR (δ, ppm, DMSO-d_6): 6.34 (d, 1H, $H_{Py,5}$, J = 7.5 Hz), 6.98 (t, 1H, $H_{arom,Ph',4}$, J = 7.5 Hz), 7.13 (d, 2H, $H_{arom,Ph,3+5}$, J = 8.8 Hz), 7.29 (t, 2H, $H_{arom,Ph',3+5}$), 7.46 (d, 2H, $H_{arom,Ph',2+6}$), 7.53 (d, 2H, $H_{arom,Ph,2+6}$), 7.76 (d, 1H, $H_{Py,6}$), 8.67 (s, 1H, $NH_{urea,1}$), 8.76 (s, 1H, $NH_{urea,3}$), 11.19 (s, 1H, NH_{Py3}), 11.35 (s, 1H, NH_{Py2}). LC−MS: m/z 362 (M^+ + H, 100). HRMS: m/z calcd for $C_{19}H_{15}N_5O_3$ [M + H]$^+$, 362.1248; found, 362.1241.

1-(4-Chlorophenyl)-3-(4-(2-oxo-2,3-dihydro-1*H*-imidazo[4,5-*b*]pyridin-7-yl-oxy)phenyl)urea (5c). A mixture of *p*-chlorophenylisocyanate (24.5 mg, 0.16 mmol) and 7-(4-aminophenoxy)-1*H*-imidazo[4,5-*b*]pyridin-2(3*H*)-one (**9**) (30 mg, 0.12 mmol) in anhydrous THF (1.5 mL) was stirred at room temperature for 14 h. The solvent was evaporated, and the solid residue was washed with Et_2O to afford the title compound (44 mg, 91%) as an off-white solid. ^{1}H NMR (δ, ppm, DMSO-d_6): 6.33 (d, 1H, $H_{Py,5}$, J = 6.0 Hz), 7.12 (d, 2H, $H_{arom,Ph,3+5}$, J = 8.9 Hz), 7.32 (d, 2H, $H_{arom,Ph,2+6}$,

Table 2. BRAF Inhibitors with Amide Linker B−C

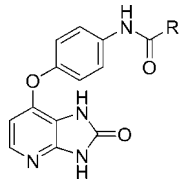

Compound	R	BRAF IC_{50} (μM)	SRB GI_{50} (μM)
27a		>100	>100
27b	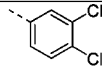	15.9	8.1
27c	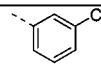	17.2	22
27d		14	18
27e	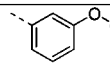	>100	>100
27f	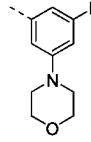	>100	44
28a		16.7	73
28b	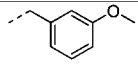	>10	40
28c	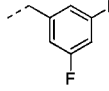	>100	29
28d	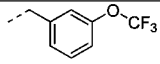	>10	23.9
28e	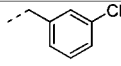	>10	>5

Table 3. BRAF Inhibitors with Sulfonamide Linker B−C

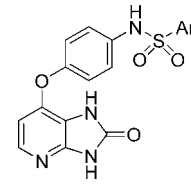

Compound	R	BRAF IC_{50} (μM)	SRB GI_{50} (μM)
29a	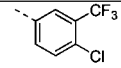	>100	40.3
29b		0.85	62.7
29c		>100	39
29d	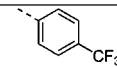	>100	41
29e		>100	ND
29f		12.2	15.6
29g		32.5	62

Table 4. Pharmacokinetics Data for Selected Inhibitors

compound	tissue	C_{max} (nmol/L)	AUC (h·nmol/L)	$T_{1/2}$ (h)	CL (L/h)
5a	plasma	1057	718	0.80	0.117
	tumor	207	468	1.24	0.160
5o	plasma	2454	3256	2.58	0.017
	tumor	1152	4504	9.72	0.006
5q	plasma	3230	16382	4.72	0.050
	muscle[a]	8078	9461	4.35	0.009

[a] Muscle was used as a surrogate for tumor.

J = 8.9 Hz), 7.50 (~t, 4H, $H_{arom'}$), 7.75 (d, 1H, $H_{Py,6}$, J = 6.0 Hz), 8.82 (bs, 1H, NH_{urea}), 8.85 (bs, 1H, NH_{urea}), 11.17 (bs, 1H, NH_{Py3}), 11.34 (bs, 1H, NH_{Py2}). LC−MS: m/z 396 (M^+ + H, 100). HRMS: m/z [M + H]$^+$ calcd for $C_{19}H_{15}ClN_5O_3$, 396.0863; found, 396.0866.

Using the same procedure the following compounds were synthesized: **5e−g, 5k−x**.

1-(3-Chloro-5-(trifluoromethyl)phenyl)-3-(4-(2-oxo-2,3-dihydro-1*H*-imidazo[4,5-*b*] pyridin-7-yl-oxy)phenyl)urea (5d). A mixture of phenyl 3-chloro-5-(trifluoromethyl)phenyl-carbamate (50 mg, 0.15 mmol) and 7-(4-aminophenoxy)-1*H*-imidazo[4,5-*b*]pyridin-2(3*H*)-one (**9**) (30 mg, 0.12 mmol) in anhydrous DMSO (1 mL) was stirred at 85 °C for 2 h. After cooling, the solution was diluted with AcOEt (10 mL), washed with H_2O (2 × 10 mL) and brine (10 mL). The solvent was evaporated and the residue was washed with Et_2O to afford the title compound as a white solid (48 mg, 85%). ^{1}H NMR (δ, ppm, DMSO-d_6): 6.32 (d, 1H, $H_{Py,5}$, J = 6.0 Hz), 7.12 (d, 2H, $H_{arom,Ph,3+5}$, J = 9.0 Hz), 7.39 (bs, 1H, $H_{arom',4}$), 7.55 (d, 2H, $H_{arom,Ph,2+6}$, J = 9.0 Hz), 7.75 (d, 1H, $H_{Py,6}$, J = 6.0 Hz), 7.84 (m, 2H, $H_{arom',2+6}$), 9.27 (bs, 1H, NH_{urea}), 9.51 (bs, 1H, NH_{urea}), 11.21 (bs, 1H, NH_{Py3}), 11.38 (bs, 1H, NH_{Py2}). LC−MS: m/z 464 (M + H, 100). HRMS: m/z [M + H]$^+$ calcd for $C_{20}H_{14}ClF_3N_5O_3$, 464.0737; found, 464.0745.

Using the same procedure the following compounds were synthesized: **5h**, **5i**,**j**.

***N*-(4-(2-Oxo-2,3-dihydro-1*H*-imidazo[4,5-*b*]pyridin-7-yl-oxy)-phenyl)benzamide (27a).** 7-(4-Aminophenoxy)-2,3-dihydro-2-oxo-1*H*-imidazo[4,5-*b*]pyridine (**9**) (30 mg, 0.13 mmol) and triethylamine (22.3 μL, 0.16 mmol) were mixed in dry THF (3 mL), and benzoyl chloride (19.0 μL, 0.16 mmol) was added. This mixture was heated to reflux for 20 h, and subsequently the solvent was evaporated under vacuum. The obtained residue was dissolved in acetone (2 mL), and upon addition of H_2O a solid precipitated. This solid was collected, washed with water (2 × 2 mL) and Et_2O (2 × 2 mL) and dried. The title compound was obtained as a light brown solid (44 mg, 80%). ^{1}H NMR (δ, ppm, DMSO-d_6): 6.39 (d, 1H, $H_{Py,5}$, J = 5.0 Hz), 7.19 (d, 2H, $H_{arom,Ph,3+5}$, J = 7.5 Hz), 7.51−7.63 (m, 3H, $H_{arom,Ph',3+4+5}$), 7.78 (d, 1H, $H_{Py,6}$), 7.86 (d, 2H,

$H_{arom,Ph,2+6}$), 7.97 (d, 2H, $H_{arom,Ph',2+6}$), 10.36 (s, 1H, NH_{amide}), 11.22 (s, 1H, NH_{Py3}), 11.39 (s, 1H, NH_{Py2}). LC−MS: *m*/*z* 347 (M + H, 100). HRMS: *m*/*z* $[M + Na]^+$ calcd for $C_{19}H_{14}N_4O_3$, 369.0958; found, 369.0954.

Using the same methodology the following compounds were synthesized: **27b**−**d**, **27f**, **28a**−**c**.

***N*-(4-(2-Oxo-2,3-dihydro-1*H*-imidazo[4,5-*b*]pyridin-7-yl-oxy)-phenyl)-3-(trifluoromethoxy)benzamide (27e).** To 7-(4-aminophenoxy)-1*H*-imidazo [4,5-*b*]pyridin-2(3*H*)-one (**9**) (50 mg, 0.21 mmol) in anhydrous dioxane (7 mL) pyridine (38 μL, 1.3 equiv) and 3-trifluoromethyloxy-benzoyl chloride (56 μL, 0.25 mmol) were added under stirring and nitrogen atmosphere and heated for 20 h at 80 °C (block). The solvent was evaporated under vacuum and the solid residue dissolved in 10 mL of AcOEt and washed with brine (2 × 10 mL), solution of citric acid (10 mL) and brine (10 mL) again. The organic solution was evaporated under vacuum and the solid residue recrystallized from AcOEt when the title compound (18 mg, 20%, purity 91%) was obtained. ^{1}H NMR (δ, ppm, DMSO-d_6): 6.39 (d, 1H, $H_{Py,5}$, J = 5.9 Hz), 7.19 (d, 2H, $H_{arom3+5}$, J = 9.0 Hz), 7.61−7.63 (m, 1H, H_{arom}), 7.70 (t, 1H, H_{arom}, J = 8.0 Hz), 7.78 (d, 1H, $H_{Py,6}$, J = 5.9 Hz), 7.84 (d, 2H, $H_{arom,Ph,2+6}$, J = 9.0 Hz), 7.91 (s, 1H, H_{arom}), 8.02 (d, 1H, H_{arom}, J = 7.9 Hz), 10.45 (s, 1H, NH_{amide}), 11.17 (s, 1H, NH_{Py2}), 11.43 (s, 1H, NH_{Py3}). LC−MS: *m*/*z* 431.2 (M^+, 100). HRMS: (M^+) calcd for $C_{21}H_{26}N_5O_3$, 431.0967; found, 431.0967.

Using the same procedure the following compounds were synthesized: **28d**,**e**.

***N*-(4-(2-Oxo-2,3-dihydro-1*H*-imidazo[4,5-*b*]pyridin-7-yl-oxy)-phenyl)-3-(trifluoromethyl)-4-chloro-benzenesulfonamide (29a).** 7-(4-Aminophenoxy)-2,3-dihydro-2-oxo-1*H*-imidazo[4,5-*b*]pyridine (**9**) (30 mg, 0.13 mmol) was suspended in dry pyridine (3 mL), and 4-chloro-3-(trifluoromethyl)benzene sulfonyl chloride (44.4 mg, 0.16 mmol) was added. The resulting solution was stirred at room temperature for 20 h and subsequently the solvent was evaporated under vacuum. The obtained residue was dissolved in acetone (4 mL) and upon addition of H_2O a solid precipitated. The solid was collected, washed with H_2O (2 × 2 mL) and Et_2O (2 × 2 mL) and dried to give the title compound as an off-white solid (44 mg, 57%). ^{1}H NMR (δ, ppm, DMSO-d_6): 6.28 (d, 1H, $H_{Py,5}$, J = 5.8 Hz), 7.12 (s, 4H, $H_{arom,Ph}$), 7.75 (d, 1H, $H_{Py,6}$), 7.98 (s, 2H, $H_{arom,Ph'}$), 8.05 (s, 1H, $H_{arom,Ph'}$), 10.47 (s, 1H, $NHSO_2$), 11.17 (s, 1H, NH_{Py3}), 11.40 (s, 1H, NH_{Py2}). LC−MS: *m*/*z* 485 [$(M + H)^+$, 100]. HRMS: *m*/*z* $[M + H]^+$ calcd for $C_{19}H_{12}ClF_3N_4O_4S$, 485.0299; found, 485.0298.

Using the same method the following compounds were synthesized: **29b**−**g**.

^{V600E}BRAF Kinase Assay and SRB IC_{50} for BRAF Inhibitors. These assays have been described by Niculescu-Duvaz et al.[20]

Compound Metabolism. Microsomal incubations evaluating phase I metabolism were performed as previously described.[21] Compounds were incubated at 10 μM concentrations for 30 min. The reaction was stopped by the addition of methanol (3 volumes), containing roscovitine (500 nM) used as an internal standard. The parent compound and metabolites were measured by liquid chromatography mass spectrometry with electrospray in positive ionization mode on 2 instruments as previously described.[22] The chromatographic separation was achieved on a Synergi polar RP column (5 cm, 4 μm particle, 4.6 mm i.d.; Phenomenex, Cheshire, U.K.) with gradient and mass spectrometry conditions similar to those described in Nutley et al.[3]

Pharmacokinetics. Forty-eight female Crl:CD1-Foxn1nu mice bearing mutant BRAF WM266.4 tumor xenografts were utilized for the PK analysis of compounds **5a** and **5p**. Twenty-four female BALB/cAnNCrl mice at least 6 weeks of age were used for the PK analysis of compound **5q**. The mice were dosed iv (2 mg/kg, 10 mL/kg, in DMSO:Tween 20:water 10:1:89 v:v). At intervals of 5, 15, 30 min, 1, 2, 4, 6 and 24 h postdosing, 3 mice were placed under isoflurane anesthesia and blood for plasma preparation was taken by terminal cardiac puncture into heparinized syringes. Femoral muscle was also sampled from the BALB/cAnNCrl mice. Tumor samples were taken from the Crl:CD1-Foxn1nu mice. Muscle, tumor and plasma samples were snap frozen in liquid nitrogen and then stored at −70 °C prior to analysis. All procedures involving animals were performed in accordance with national Home Office regulations under the Animals (Scientific Procedures) Act 1986 and within guidelines set out by the Institute's Animal Ethics Committee and the United Kingdom Coordinating Committee for Cancer Research's *ad hoc* Committee on the Welfare of Animals in Experimental Neoplasia.[23] Plasma and tissue extractions were performed as previously described.[24] Analysis was also performed by multiple reaction monitoring of the compounds and the internal standard roscovitine on the triple quadrupole with an external calibration and 3 quality controls at levels between 10 and 10000 nM. PK parameters were derived from WinNonLin Non-Compartmental analysis (Pharsight, version 3.2).

Acknowledgment. This work is supported by Cancer Research UK (refs: C309/A2187 and C107/A10433), The Wellcome Trust, The Institute of Cancer Research and The Isle of Man Anti-Cancer Association. We acknowledge NHS funding to the NIHR Biomedical Research Centre. We thank Professors Paul Workman and Julian Blagg for helpful discussions and support.

Supporting Information Available: Experimental details of the synthesis and analytical characterization of compounds **5e**−**x**, **26**, **27b**−**d**, **27f**, **28a**−**e**, **29b**−**g**, and intermediates **2**−**4**, **6**−**25** described in this paper and purity data for the final compounds. This material is available free of charge via the Internet at http://pubs.acs.org.

References

(1) Wellbrock, C.; Karasarides, M.; Marais, R. The RAF proteins take center stage. *Nat. Rev. Mol. Cell Biol.* **2004**, *5*, 875–885.
(2) Chiloeches, A.; Marais, R. Mitogen-activated protein kinase cascades as therapeutic targets in cancer. In *Targets for Cancer Chemotherapy: Transcription Factors and Other Nuclear Proteins*; Humana Press Inc.: Totowa, NJ, 2002; pp 179−206.
(3) Kolch, W. Meaningful relationships: the regulation of the Ras/Raf/MEK/ERK pathway by protein interactions. *Biochem. J.* **2000**, *351*, 289–305.
(4) Davies, H.; Bignell, G. R.; Cox, C.; Stephen, P.; et al. Mutation of the BRAF gene in human cancers. *Nature* **2002**, *417*, 949–954.
(5) Tuveson, D. A.; Weber, B. L.; Herlyn, M. BRAF as a potential therapeutic target in melanoma and other malignancies. *Cancer Cell* **2003**, *4*, 95–98.
(6) Garnett, M. J.; Marais, R. Guilty as charged: B-RAF is a human oncogene. *Cancer Cell* **2004**, *6*, 313–319.
(7) Wellbrock, C.; Ogilvie, L.; Hedley, D.; Karasarides, M.; Martin, J.; Niculescu-Duvaz, D.; Springer, C. J.; Marais, R. ^{V599E}B-RAF is an oncogene in melanocytes. *Cancer Res.* **2004**, *64*, 2338–2342.
(8) Ikenoue, T.; Hikiba, Y.; Kanai, F.; Tanaka, Y.; Imamura, J.; Imamura, T.; Ohta, M.; Ijichi, H.; Tateishi, K.; Kawakami, T.; Aragaki, J.; Matsumura, M.; Kawabe, T.; Omata, M. Functional analysis of mutations within the kinase activation segment of B-Raf in human colorectal tumors. *Cancer Res.* **2003**, *63*, 8132–8137.
(9) Karasarides, M.; Chiloeches, A.; Hayward, R.; Niculescu-Duvaz, D.; Scanlon, I.; Friedlos, F.; Ogilvie, L.; Hedley, D.; Martin, J.; Marshall, C. J.; Springer, C. J.; Marais, R. B-RAF is a therapeutic target in melanoma. *Oncogene* **2004**, *23*, 6292–6298.
(10) Hingorani, S. R.; Jacobetz, M. A.; Robertson, G. P.; Herlyn, M.; Tuveson, D. A. Suppression of BRAF(V599E) in human melanoma abrogates transformation. *Cancer Res.* **2003**, *63*, 5198–5202.
(11) www.clinicaltrials.gov. NCT00405587: Safety Study of PLX4032 in Patients With Solid Tumors.
(12) www.clinicaltrials.gov. NCT00304525: A Study to Evaluate RAF265, an Oral Drug Administered to Subjects With Locally Advanced or Metastatic Melanoma.
(13) www.clinicaltrials.gov. NCT00451880: Study of XL281 in Adults With Solid Tumors.
(14) Ahmad, T.; Eisen, T. Kinase inhibition with BAY 43−9006 in renal cell carcinoma. *Clin. Cancer Res.* **2004**, *10*, 6388S–6392S.
(15) Eisen, T.; Ahmad, T.; Flaherty, K. T.; Gore, M.; Kaye, S.; Marais, R.; Gibbens, I.; Hackett, S.; James, M.; Schuchter, L. M.; Nathanson, K. L.; Xia, C.; Simantov, R.; Schwartz, B.; Poulin-Costello, M.; O'Dwyer, P. J.; Ratain, M. J. Sorafenib in advanced melanoma: a Phase II randomised discontinuation trial analysis. *Br. J. Cancer* **2006**, *95*, 581–586.

(16) Collins, I.; Workman, P. Design and development of signal transduction inhibitors for cancer treatment: Experience and challenges with kinase targets. *Curr. Signal Transduction Ther.* **2006**, *1*, 13–23.
(17) Veber, D. F.; Johnson, S. R.; Cheng, H.-Y.; Smith, B. R.; Ward, K. W.; Kopple, K. D. Molecular Properties That Influence the Oral Bioavailability of Drug Candidates. *J. Med. Chem.* **2002**, *45*, 2615–2623.
(18) Liao, J. J.-L. Molecular Recognition of Protein Kinase Binding Pockets for Design of Potent and Selective Kinase Inhibitors. *J. Med. Chem.* **2007**, *50*, 409–424.
(19) Wan, P. T. C.; Garnett, M. J.; Roe, S. M.; Lee, S.; Niculescu-Duvaz, D.; Good, V. M.; Project, C. G.; Jones, C. M.; Marshall, C. J.; Springer, C. J.; Barford, D.; Marais, R. Mechanism of activation of the RAF-ERK signaling pathway by oncogenic mutations of B-RAF. *Cell* **2004**, *116*, 855–867.
(20) Niculescu-Duvaz, I.; Roman, E.; Whittaker, S. R.; Friedlos, F.; Kirk, R.; Scanlon, I. J.; Davies, L. C.; Niculescu-Duvaz, D.; Marais, R.; Springer, C. J. Novel Inhibitors of B-RAF Based on a Disubstituted Pyrazine Scaffold. Generation of a Nanomolar Lead. *J. Med. Chem.* **2006**, *49*, 407–416.
(21) Smith, N. F.; Hayes, A.; Nutley, B. P.; Raynaud, F. I.; Workman, P. Evaluation of the cassette dosing approach for assessing the pharmacokinetics of geldanamycin analogues in mice. *Cancer Chemother. Pharmacol.* **2004**, *54*, 475–486.
(22) Nutley, B. P.; Raynaud, F. I.; Wilson, S. C.; Fischer, P. M.; Hayes, A.; Goddard, P. M.; McClue, S. J.; Jarman, M.; Lane, D. P.; Workman, P. Metabolism and pharmacokinetics of the cyclin-dependent kinase inhibitor R-roscovitine in the mouse. *Mol. Cancer Ther.* **2005**, *4*, 125–139.
(23) Workman, P.; Twentyman, P.; Balkwill, F. United Kingdom Co-ordinating Committee on Cancer Research guidelines for the welfare of animals in experimental neoplasia, 2nd Ed. *Br. J. Cancer* **1998**, *77*, 1–10.
(24) Raynaud, F. I.; Whittaker, S. R.; Fischer, P. M.; McClue, S.; Walton, M. I.; Barrie, S. E.; Garrett, M. D.; Rogers, P.; Clarke, S. J.; Kelland, L. R.; Valenti, M.; Brunton, L.; Eccles, S.; Lane, D. P.; Workman, P. In vitro and in vivo pharmacokinetic-pharmacodynamic relationships for the trisubstituted aminopurine cyclin-dependent kinase inhibitors olomoucine,bohemine and CYC202. *Clin. Cancer Res.* **2005**, *11*, 4875–4887.

JM801509W